Direct Effects of Solar Irradiance on a Concentrated Solar Powered Water-Ammonia Absorption Refrigerator

Behnam Mostajeran Goortani *‡, Fatemeh Babaei **, Ali Akbar Alemrajabi ***, Mojtaba Mostajaboddavati****

*& ** Renewable Energies Engineering Department, Faculty of Advanced Sciences and Technologies, University of Isfahan, Isfahan, Iran

*** Department of Mechanical Engineering, Isfahan University of Technology, Isfahan, Iran

**** Department of Physics, University of Isfahan, Isfahan, Iran

‡ Corresponding Author; First Author, Postal address, Tel: +98 9103450496,

Fax: +98 3137932129, b.mostajeran@ast.ui.ac.ir

Received: 01.09.2019 Accepted:05.11.2018

Abstract- A comprehensive model with respect to the "variable with time" nature of sun thermal energy is developed to assess the direct effects of solar irradiance on the operation and process parameters of a concentrated solar powered single effect ammonia-water absorption refrigerator. This model is composed of coupling three models for the solar collector, heat storage, and absorption refrigerator. The effects of collector area, solar irradiance, and flow rate of hot oil/salt melt variations during the day are calculated through this model. This model is based on the Bird's clear sky irradiation model, validated against the solar irradiance experimental data. The refrigerator model is based on two-phase, two components mass and energy balances for the elements of the refrigeration cycle. A small scale solar concentrated collector is ıntroduced, where salt melts in the temperature range of 215 ^{o}C to 334.5 ^{o}C (suitable temperature range in the generator of water-ammonia refrigerators) can be utilised, and an overall collector efficiency of 57.8% is determined. To assure the steady operation of the refrigerator during the day and night with a thermal storage capacity for 12 hours and considering the heat losses thereof, a total capacity of 280 kg to 380 kg thermal storage medium and a collector surface area of 6.3 to 18 m^2 is required. By changing the mass flow rate of salt melt in the collector from 0.005 kg/s to 0.025 kg/s the drastic effects of solar energy change on the parameters of the refrigeratore can be prevented.

Keywords Absorption refrigerator; concentrated solar heat; storage; water-ammonia.

1. Introduction

A significant amount of electrical energy is consumed for air conditioning and refrigeration systems in the building and industrial sectors, particularly in warm climate areas. In Saudi Arabia this amount accounts for about 60% of the total energy consumption, attributed to the building sector [Said et al., (2012)]. In Iran, this amount accounts for about 7.5 GWh, attributed to the building sector. The energy demand increases during the day as the weather temperature and solar irradiance increases. Therefore, any improvement and savings in the cooling systems by replacing the electricity with solar energy is of vital importance.

There exist many experimental and theoretical studies in this respect, particularly water-ammonia systems [Lostec et al., (2012) and (2013), Benhmidene et al., (2016)]. Zohar et

al., (2005) studied a fossil fuel based, Sevrel-Electroloux refrigerator and revealed that the best performance of the refrigerator is yield with a rich solution of 20% to 30% ammonia and a weak solution of 10% ammonia. They compared He and H_2, as pressure balancing inert gases, and found that the coefficient of performance (COP) utilizing He is about 40% greater than that of H_2. Tzivanidis and Bellos (2016), studied parametrically a solar refrigeration system powered by parabolic trough collectors and showed that for 3 kW cooling capacity at 10 ^oC and ambient temperatures of the city of Athens, a 51 m^2 collector is required.

Kong et al., (2010) modeled a 2 kW refrigerator and revealed that an increase in generator thermal load, from 4.8 kW to 6.5 kW, increases the cooling capacity from 2.2 to 3.0 kW. Their model approximates the experimental data with 75% accuracy. Ozorgen et al., (2012) modeled a 2.5 kW evacuated tube, solar, absorption refrigerator. The hourly variations of solar radiation and atmospheric temperature for Adana province in Turkey is considered. Based on their findings, the needed collector area is between 25 m^2 and 41 m^2, depending on the hour and the climatic conditions of the given day.

Some researchers like Helm et al., (2014), Winston et al., (2014), and Berger et al., (2012) studied larger solar cooling systems. Berger et al., (2012) assessed a standard solar system for industrial cooling applications. Instead of one large chiller, two smaller water-ammonia absorption chillers with a rated thermal COP of 0.6, total cooling power of 24 kW, and operating temperature of 450 K were chosen to study part-load behavior in the cascaded operation. Four ice storages with a total volume of 1.200 m^3 and a corresponding melting thermal capacity of 110 kWh was applied to enable peak shifting. Pablo et al., (2010) studied a hybrid system composed of a double-effect absorption chiller of 174 kW nominal cooling capacity, powered by: 1) a pressurized hot water flow delivered by means of a 352 m^2 solar field of a linear Fresnel collector and 2) a direct-fired natural gas burner. The absorption chiller operates with a daily average COP of 1.1–1.25, where the solar energy presented 75% of the generator's total heat input. Al-Alili et al., (2012) assessed the feasibility of utilizing a solar powered absorption cycle subject to Abu Dhabi's (UAE) weather conditions. The solar air conditioner system had a specific collector area of 6 m^2/kWc and a specific tank volume of 0.1 m^3/kWc.

With respect to the nature of renewable sources of energy subject to 'vary with time' [Hosseini et al., (2016), Agrouaz et al., (2017), Solak at al., (2015)], particularly sun thermal energy, it is necessary to utilize and store the energy for night consumption. For this purpose, a solar absorption chiller is usually composed of three components: solar collector, thermal storage, and absorption cycle.

The objective here is to predict the direct effects of solar intensity variations, during the day and throughout the year, on concentrated solar thermal refrigerator parameters. The absorption cycle model developed in this study is validated against the available experimental data in the literature for the Servel-Electrolux absorption cycle, a 50-100 W cooling capacity refrigerator. This solar irradiance model is based on the Bird's clear sky model. The effects of the collector area and solar irradiance variations on the cooling capacity, generator load and temperature, and heat storage tank mass are assessed here. The advantages of a thermal heat storage system in terms of absorbing drastic solar energy change and storing the energy for working overnight and working during cloudy hours are assumed and calculated in a quantitative manner.

2. Description of the concentrated solar powered absorption refrigerator

The role of thermal energy in the generator of absorption refrigeration systems is similar to that of electricity in the compressor of the vapor compression systems. The working fluid in the absorption system of this study is water-ammonia mixture: water as the absorbing medium and ammonia as the refrigerant.

The schematic of a water-ammonia absorption cycle refrigerator powered by concentrated solar radiation is shown in Fig.1. The thermal energy is received by a circulating heat transfer fluid (hot oil/salt melt) and is sent to the generator of the absorption refrigerator. In the generator, the water-ammonia mixture is heated, by the fluid, to produce ammonia rich vapor and ammonia weak liquid.

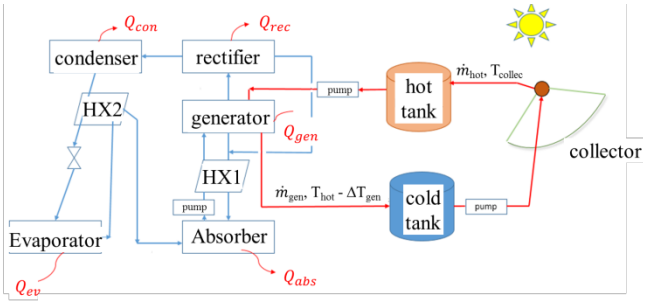

Fig. 1. A concentrated solar powered absorption refrigerator.

From the generator, the ammonia-rich vapor flows to the rectifier at high pressure and high temperature, while the water vapor fraction is condensed and returned back to the absorber. The ammonia vapor, first flows from the rectifier to the condenser and is cooled to a medium temperature liquid; next, the liquid enters the adiabatic expansion valve and is flashed to a vapor-liquid mixture at a lower pressure and temperature. This mixture then flows to the evaporator where heat (Q_{ev}) is absorbed and a low pressure and temperature vapor is produced. To complete the cycle, the vapor undergoes a thermo-chemical compression. The vapor is absorbed into a weak ammonia liquid mixture. The resultant liquid, rich in ammonia, is then sent to the generator and this cycle repeats. Two heat exchanges, the HX1 and HX2, recover the internal energy of the cycle and increase the cycle efficiency.

The rectifier plays a critical role in the refrigeration cycle. It refines ammonia stream from water vapor. Without a rectifier, the evaporator may be blocked, because of existing water vapor in the ammonia stream. By cooling the generator vapors, ammonia with higher purity is yielded. The condenser is a shell and tube heat exchanger. The ammonia-rich mixture enters the condenser and loses its internal

energy. The expansion valve process is isenthalpic through which the outlet stream temperature suddenly drops (Joule-Thomson effect). The outlet stream from this valve is a liquid–vapor mixture. The liquid stream from the generator, named the weak solution, flows to the absorber, and after absorbing the vapor coming from the evaporator, it is pumped to the generator.

For steady operation of the absorption refrigerators, a heating source with sufficient thermal power and temperature (minimum 570 K) is required. Busso et al., (2011) tested a 2 m^2 parabolic collector connected to a Sevrel-Electroloux refrigerator and found that the diameter and area of the collector are not sufficient to provide the required temperature for permanent operation of the refrigerator.

3. Modelıng the concentrated solar powered absorptıon refrıgerator

Here, the developed model is composed of a sun tracing solar collector with thermal heat storage connected to a water-ammonia absorption refrigerator. The gPROMS software is an advanced modeling tool applied in modeling mass and energy balances of the equipment and processes under transient or steady state conditions. This software is mainly utilized in oil and gas research sector, Mostajeran B. et. al., (2015). This software is equation-oriented and allows user to write appropriate equations and solve them in a simultaneous manner by assuming variable physical and thermodynamic properties of the materials.

The equations applied in calculating these properties for the pure components and mixtures, in vapor and liquid phases, are all presented as functions of pressure, temperature, and components fractions. In the calculation of enthalpy of water-ammonia mixture, the enthalpy is written as a function of temperature, pressure, and components fractions, (T, P, X). The mass and energy balances are presented and solved in gPROMS, simultaneously. Physical and thermodynamic properties of the liquid and vapor phases are calculated through the Multiflash which is a physical and thermodynamic property calculation software [Schmitz and Ulrich, (2017)].

In this model, the direct effects of solar irradiance variations during the day on the energy and material balance of generator, condenser, expansion valves, pump, evaporator, absorber, and heat exchangers are involved. The inputs of this model are: high and low pressures, water ammonia flow rate and mole fraction, temperature, rich solution mole fraction, refrigerator capacity, geographical location, time and the given day. The required collector area, heat storage tank masses, generator power, COP, inlet and outlet streams, and temperatures and component compositions are calculated through this model. A diagram of the three models and their inter connections are outlined in Fig. 2. Multiflash is utilized for the calculation of physical and thermodynamic properties.

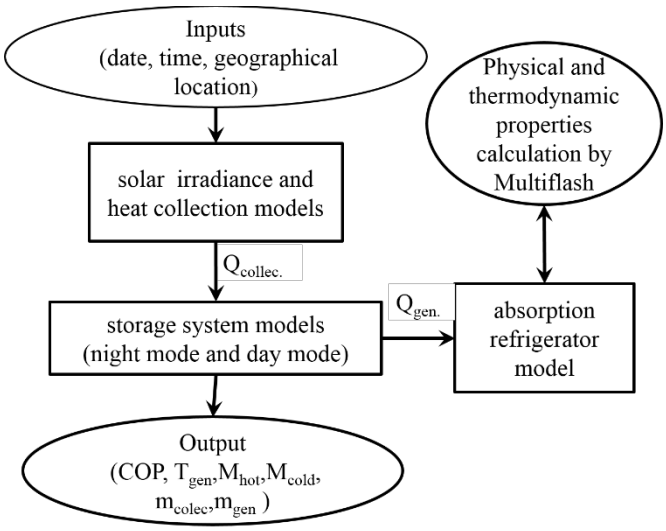

Fig. 2. Structure and communication between the models in concentrated solar powered refrigerator

3.1 Solar irradiance and collector models

The solar collector model is composed of the collector model and the solar irradiance model. There exist many theoretical end experimental equations for the calculation of solar irradiance [e.g. Duffie and Beckman, (2013), Ashjaee et. al., (1993), K. Qiu, and Thorsteinson, (2014)]. In this study the Bird's clear sky model tabulated in Gueymard, (2012), is applied.

3.2. Absorption refrigerator model

In the refrigerator model the following assumptions are made:

a) Processes is steady state

b) Heat losses are negligible

c) Condenser, absorber, and generator work under thermodynamic equilibrium conditions

d) Expansion valve works under adiabatic conditions and vapour and liquid outlet streams are at equilibrium.

e) The pumping effect of the generator on the mass and energy balance is negligible

f) There exist two pressure levels in the absorption cycle, high pressure and low pressure. Generator, rectifier, and condenser work under high pressure; while, the expansion valve, evaporator, and absorber, work under low pressure.

The two-component two-phase mass and energy balance equations for the generator, rectifier, condenser, evaporator, and absorber are tabulated in Table 1., where, *L, V, x, y, h,* Q_{gen} and *i*, are the liquid molar rate, vapor molar rate, liquid mole fraction, vapor mole fraction, molar enthalpy, generator duty, and component number, respectively. Subscripts *in* and *out* refer to the inlet and outlet streams. The sum of all liquid and vapor mole fractions should be 1. Subscripts *gen, rec,*

con, expv, evp, abs, hx_1, and hx_2 refer to the generator, rectifier, condenser, expansion valve, evaporator, absorber, heat exchanger 1, and heat exchanger 2, respectively.

Table 1. Two-component two-phase mass and energy balances on the absorption cycle

Generator	$L_{in\_gen} = L_{out\_gen} + V_{out\_gen}$ $x_{in-gen}(i) * L_{in\_gen} = x_{out\_gen}(i) * L_{out\_gen} + y_{out\_gen}(i) * V_{out\_gen}$ $x_{out-gen}(i) = \alpha_i * y_{out_{gen}}(i)$ $Q_{gen} = L_{in_{gen}} * Liq.Entlpy(T_{in-gen}, P_{gen}, x_{in-gen}) - V_{out-gen} * Vap.Entlpy(T_{gen}, P_{gen}, y_{out-gen})$ $-L_{out-gen} * Vap.Entlpy(T_{gen}, P_{gen}, y_{out-gen})$
Rectifier	$V_{in\_rec} = L_{out\_rec} + V_{out\_rec}$ $y_{in-rec}(i)V_{in_{rec}} = x_{out-rec}(i) * L_{out_{rec}} + y_{out-rec}(i) * V_{out_{rec}}$ $Q_{rec} = L_{in-rec} * Liq.Entlpy(T_{in-rec}, P_{gen}, x_{in-rec}) - V_{out-rec} * Vap.Entlpy(T_{rec}, P_{gen}, y_{out-rec})$ $-L_{out-rec} * Vap.Entlpy(T_{rec}, P_{gen}, y_{out-rec})$
Condenser	$V_{in\_con} = L_{out\_con}$ $y_{in\_con}(i) = x_{out\_con}(i)$ $Q_{con} = V_{in-con} * Vap.Entlpy(T_{in-con}, P_{gen}, y_{in-con}) - L_{out-con} * Liq.Entlpy(T_{out-con}, P_{gen}, y_{out-con})$
Expansion valve	$L_{in\_exp} = L_{out\_exp} + V_{out\_exp}$ $x_{in-exp}(i) * L_{in-exp} = x_{out-exp}(i) * L_{out-exp} + y_{out-exp} * V_{out-exp}$ $Q_{in\_exp} = L_{in\_exp} * Liq.Entlpy(T_{in-exp}, P_{gen}, x_{in-exp}) - L_{out-exp} * Liq.Entlpy(T_{out-exp}, P_{abs}, x_{out-exp}) - V_{out-exp} * Vap.Entlpy(T_{out-exp}, P_{abs}, y_{out-exp})$
Evaporator	$L_{in\_ev} + V_{in\_ev} = V_{out\_ev}$ $x_{in-ev}(i) * L_{in-ev} + y_{in-ev}(i) * V_{in-ev} = y_{out-ev} * V_{out-ev}$ $Q_{ev} = L_{in\_ev} * Liq.Entlpy(T_{in-ev}, P_{abs}, x_{in-ev}) + V_{in-ev} * Vap.Entlpy(T_{in-ev}, P_{abs}, y_{in-ev}) - V_{out-ev} * Vap.Entlpy(T_{out-ev}, P_{abs}, y_{out-ev})$
Absorber	$V_{in\_abs} = L_{out\_abs} - L_{in-abs}$ $y_{in-abs}(i) * V_{in-abs} = x_{out-abs}(i) * L_{out-abs} - x_{in-abs} * L_{in-abs}$ $Q_{abs} = V_{in\_abs} * Vap.Entlpy(T_{in-abs}, P_{abs}, y_{in-abs}) - L_{in\_abs} * Liq.Entlpy(T_{in-abs}, P_{abs}, x_{in-abs}) + L_{out-abs} * L_{out\_abs} * Liq.Entlpy(T_{abs}, P_{abs}, x_{out-abs})$
Heat Exchangers	$L_{out-con} * [Liq.Entlpy(T_{out-con}, P_{gen}, x_{out-con}) - Liq.Entlpy(T_{out-hx2}, P_{gen}, x_{out-con})] = V_{out-ev} * [Vap.Entlpy(T_{in-abs}, P_{abs}, y_{in-abs}) - Vap.Entlpy(T_{out-ev}, P_{abs}, y_{out-ev})]$ $L_{out-abs} * [Liq.Entlpy(T_{out-abs}, P_{abs}, x_{out-abs}) - Liq.Entlpy(T_{out-hx1}, P_{gen}, x_{out-abs})] = L_{out-gen} * Liq.Entlpy(T_{out-gen}, P_{gen}, x_{out-gen}) + L_{out-rec} * Liq.Entlpy(T_{out-rec}, P_{gen}, x_{out-rec}) - (L_{out-gen} + L_{out-rec}) * Liq.Entlpy(T_{in-abs}, P_{gen}, x_{in-abs})$

Heat exchanger 1 (HX1) cools the outlet stream of the generator and the rectifier; heat exchanger 2 (HX2) recovers the internal energy of the system. Heat exchanger 2 cools the outlet stream of the condenser and raises the temperature of the vapor stream of the evaporator. It is assumed that the liquid streams of the generator and condenser are cooled to a certain temperature levels, ΔT_hx1 , and ΔT_hx2, respectively. The equations applied

in calculating ΔT_hx1 and ΔT_hx2 through ε-NTU method are depicted from Incorpera and DeWitt, (1990).

3.3. Solar heat storage model

The heat storage system is composed of two hot and cold tanks, one generator, and a collector receiver, Fig.1. Hot oil/salt melt from the cold tank is heated in the collector receiver at T_{col} and is pumped to and stored in the hot tank. The hot oil/salt melt is then pumped to the generator, where it loses its sensible heat and is stored in the cold tank at temperature T_{hot}-ΔT. The differential equations applied in describing mass and energy balances in the storage tanks are tabulated in Table 2. The parameters M_{hot}, T_{hot}, M_{cold}, and T_{cold} are the mass and temperature of the hot tank and mass and temperature of the cold tank, respectively. The parameters $\dot{m}_{col}$ and $\dot{m}_{gen}$ are the hot oil/salt melt mass flow rates in the collector and generator, respectively. In the Table, ω_{sunset} is the sun set hour angle in degrees and t_{sunset} and $t_{sunrise}$ are the solar sunset and sunrise times, respectively.

Table 2. Mass and energy balances for solar heat collection storage model.

$Q_{gen} = Area * \eta * I_b$
$\dot{m}_{gen} - \dot{m}_{col} = dM_{cold}/dt$
$\dot{m}_{col} - \dot{m}_{gen} = dM_{hot}/dt$
$\frac{d(M_{hot} * Liq.Entlpy(T_{hot}, P))}{dt} = \dot{m}_{col} * Liq.Entlpy(T_{col}, P) - \dot{m}_{gen} * Liq.Entlpy(T_{gen}, P)$
$\frac{d(M_{cold} * Liq.Entlpy(T_{cold}, P))}{dt} = \dot{m}_{gen} * Liq.Entlpy(T_{hot} - T_{cold}, P) - \dot{m}_{col} * Liq.Entlpy(T_{cold}, P)$
$\int_{t_{sunrise}+1}^{t_{sunset}-1} I_b * \eta * Area * Q_{gen} dt = 24 * 3600 * Q_{gen}$
$\dot{m}_{col} * c_p * (T_{col} - T_{cold}) = I_b * \eta * Area$
$\omega_{sunset} = Acos(-tan(r * \delta) * tan(r * \phi))/r$
$t_{sunset} = 12 + \omega_{sunset}/15$, $t_{sunrise} = 12 - \omega_{sunset}/15$
$M_{cold} + M_{hot} = \dot{m}_{gen} * (t_{sunrise} - t_{sunset} - 2) * 3600$

To solve the differential equations tabulated in Table 2, initial conditions are necessary. This model is run in the night and day modes. The initial conditions of mass and temperature in the hot and cold tanks in the night mode is equal to the final conditions of mass and temperature in the hot and cold tanks in the day mode. The collector overall efficiency is assumed 70% [Duffie and Beckman, (2013)]. To intoduce a small scale solar concentrated collector in the temperature range of 200 °C to 400 °C and to determine the overall collector efficiency and apply it in the model, following experiment is repeated for two times.

An off-center parabolic dish collector, designed and fabricated at University of Isfahan, Iran, capable of increasing the temperature by more than 100 K with a collector area of around 1.4 m^2, Fig. (3). Diameter of the aperture core at the focal area is 10 cm. To focus the sun accurately on the receiver tracking is made every 30 seconds, manually, in horizontal and vertical directions. To overcome practical restrictions that might be caused by hot oil at 573 K plus, salt melt mixtures like $KNO_3/NaNO_3/NaNO_2$, are applied [Mostajeran Goortani et al., 2017, Messadi and Timoumi, (2018)]. The receiver of this collector, a laboratory made receiver, consists of three vacuum tube glass solar water heaters of 60 cm height and 4 cm diameter attached together and insulated totally except for the lower front, Fig. (3). A thermometer with data logger (model AZ instruments, Taiwan) with a type K thermocouple and with a precision ±2 °C is installed to record the temperature.

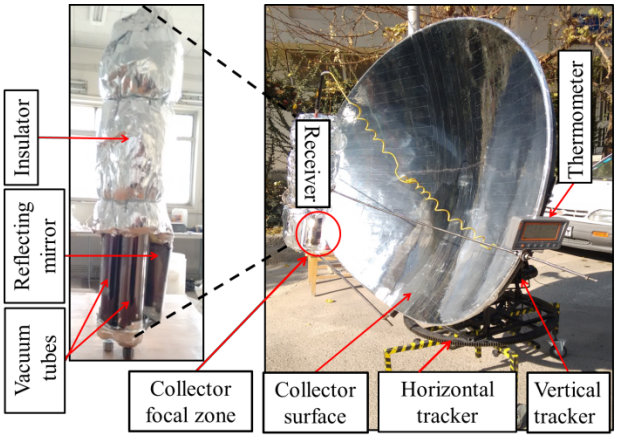

Fig. 3. Experimental set-up applied to measure overall collector efficiency in salt melt heating.

To fill the receiver tubes, first a salt mixture ($NaNO_3$, KNO_3, and $NaNO_2$) of 3450 g with a weight percentage of 7%, 44%, and 49%, respectively, is melted at around 145 °C and heated up to 215 °C and poured into the receiver tubes. The experiment is run for 30 minutes in December, 16th (2017), noon time. The final temperature of the tubes rose to 334.3 °C, thus is 119.3 °C above the initial temperature.

Total absorbed heat by the receiver, Q_{rec} , is expressed as follows:

$$Q_{rec} = (m_{melt}*Cp_{melt}*\Delta T + m_{receiver}*Cp_{receiver}*\Delta T)/t = (3.450\ kg*1521\ KJ/kg.^oC*(334.3 - 215)^oC + 2.520\ kg*845\ KJ/kg.^oC*(334.3 - 215)^oC)/(30*60s) = 626020.785 + 254037.42 = 925422.03\ J = 488.92\ W \pm 5 \quad (1)$$

To measure direct normal irradiance on the collector, a solar power meter (model TES 1333, Taiwan, precision: 0.1 W/m^2) is applied to measure global radiation. Diffuse and reflected radiation components are then subtracted from the global component [Salimian et al. (2017)]. Concentrated solar collector efficiency depends on collector design and many process parameters [Ahmed et al. (2015)]. To determine the collector overall thermal efficiency, η, as follows:

η = (total absorbed thermal power) / (available solar power) = 488.92 / (604.3 W/m^2*1.4m^2)
= 57.8±0.5 % (2)

Through more experiments and better receiver designs this 57.8% can be increased to 60% or even higher in order to promote the overall collector efficiency. This experiment is run with static salt melt. In practical continuous operation, due to higher heat transfer coefficient higher efficiency is obtained.

The absorption refrigerator model is compared with the available data from the literature for a 50 - 100 W cooling capacity Sevrel-Electrolux refrigerator [Busso et al., (2011)]. The model results are compared with time average experimental data, as observed in Table 3. The generator duty together with the generator and rectifier temperature is predicted well through this model. The difference between COPs may be attributed to heat loss neglection in the generator and the assumption of thermodynamic equilibrium state in both the generator and absorber. According to the content of Table 3. this model is a reliable one for prediction of different parameters.

Table 3. Comparison of this model with experimental data for Servel-Electrolux refrigerator (P_{gen}=2.5MPa, P_{abs}=80 KPa, x_{rich}=0.3, m_{rich}= 0.00016(kg/s), m_{weak}=0.00013(kg/s)

	Generator duty (W)	Generator temp. (K)	Rectifier temp. K)	COP
This model	150	444	335	0.15
Busso et al. [11]	140	448	332.6	0.19

4. Result and discussion

The purpose of the heat storage tanks is to act as: 1) high solar energy intensities' absorber and 2) storage of energy surplus during the sunny hours for cloudy hours or night that is, supplying the non-stop energy demand. To express the quantitative contribution of the storage tanks, the direct changes in the required collector area, generator load and temperature, and cooling capacity are calculated and presented for two cases of with and without employing storage tanks.

4.1. Direct effects of solar irradiance without heat storage

There exists a direct relation between radiation intensity and heat input to the generator. The effects of radiation intensity on the generator duty and temperature, at three collector areas of 0.58 m^2, 0.45 m^2, and 0.30 m^2 are illustrated in Fig. 4. At 0.45 m^2, when the intensity increases from around

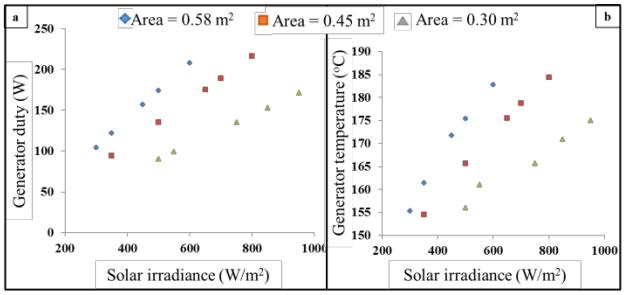

Fig. 4. Effect of radiation intensity on: (a) the generator duty, and (b) temperature. (Operating conditions: P_{high} = 2.5 MPa, P_{low} = 80 kPa, X_{rich}= 0. 30, m_{weak} = 0.00016 kg/s, T_{ev} = 263 K, T_{amb}=298.15 K)

400 W/m^2 to 800 W/m^2, the generator duty (Fig. 4-a) increases from 120 W to 220 W; while the temperature (Fig. 4-b) increases from 440 K to 463 K.

The evaporator cooling capacity increases as the solar intensity increases. The effect of solar intensity at three collector areas of 0.3m^2, 0.45m^2, and 0.58m^2 is illustrated in Fig. 5. The input conditions are tabulated in Table 3. At 0.45 m^2, the cooling capacity increases from around 15 W to about 75 W, while radiation intensity increases from around 500 W/m^2 to 800 W/m^2. Increasing the collector area has a significant effect on the cooling capacity, because of an increase in both the generator's heat input and its temperature at the same time.

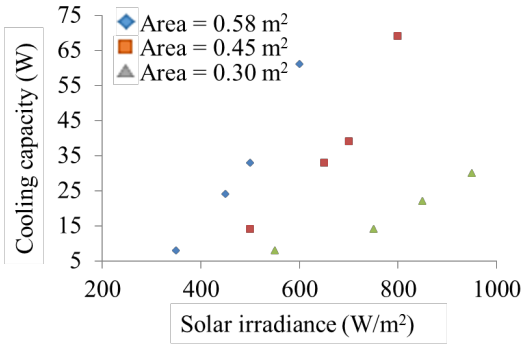

Fig. 5. Effect of radiation intensity on the evaporator cooling capacity

It is important that the data of this figure can be used to estimate the collector area required to reach a given cooling capacity. For example, at a daily average solar radiation of 470 W/m^2 according to Figure 5, an area of 0.58 m^2 is required to ensure sufficient cooling capacity of 35W. However, the peak of solar irradiation during a day, which is between 600 and 900 W/m^2, may result high temperature in the generator and this may introduce practical restrictions in using the necessary equipment. At a constant ambient temperature, as the solar intensity increases, the generator duty, and the generator temperature increase; consequently, COP and the cooling capacity increase.

As observed in Fig. 4 and Fig. 5, the refrigerator process parameters undergo a drastic change as a result of variations in solar irradiance during a day. Applying a thermal heat storage system can overcome the operational drawbacks related to these changes and may assure a steady operation of a solar refrigerator.

4.2. Direct effects of solar irradiance in the presence of heat storage

The results of the previous section (solar refrigerator without the heat storage) showed that as a result of significant increase from morning to noon and again significant decrease from noon to evening in solar irradiance, there occur significant changes in the generator temperature, evaporator capacity and generator duty. To absorb drastic changes in related parameters and to store thermal energy for overnight operation of the refrigerator, two hot and cold tanks are added to the system. During the day, hot oil/salt melt from the cold tank flows to the collector and then to the hot tank; during the night, hot oil/salt melt leaves the hot tank and enters the cold tank after its thermal energy is consumed partly by the generator [Naranjo-Mendoza et al., (2013), Martinkauppi et al. (2018)]. The parameters applied to run the solar refrigerator model with storage tanks are tabulated in Table 4. For the storage time, it is assumed that the collector starts to operate one hour after the sunrise and stops one hour before the sunset.

The generator mass flow is assumed constant and calculated from $Q = \dot{m}_{col} * c_p * \Delta T$. The collector mass flow rate is variable during the day and is controlled in a manner as to keep the outlet stream from the collector at a constant temperature of 673 K. The hourly and daily variation of system performance parameters during different seasons are obtained and shown in this section.

Table 4. Parameters used in the solar refrigerator model with two tanks heat storage

Parameter	Value
Heat collection and storage	
Collector area (m^2)	6.3 - 18
Storage time (hr)	$t_{sunrise}$-t_{sunset} - 2
Collector temperature (K)	673
Temperature drop across the generator (K)	100
Hot tank temperature (K)	673
Cold tank temperature (K)	573
Absorption refrigerator	
Generator pressure (MPa)	2.5
Absorber pressure (kPa)	80
Generator temperature (K)	413-453
Total required heat (including total heat losses and generator heat input) (kW)	1

The results of variations in tanks' temperatures for the first days of winter, spring and summer are shown in Figs. 6-a, 6-b, and 6-c, respectively. The day and night mode of this model is sunrise +1 and sunset-1 hours.

Collector surface area and salt melt mass required to supply the energy need of the generator in 24 hrs, for the designated three days, are tabulated in Table 5. By moving from winter to summer, the required collector area and tank storage capacity decreases from 18 m^2 to 6.3 m^2 and from 380 kg to 280 kg respectively, due to an increase in average solar irradiance and day length.

Table 5. gPROMS model results for three days of the year

Day of the year	Sunrise	Sunset	Day length (h)	I_{avg} (W/m^2)	Tank mass (kg)	Collector area (m^2)
Winter 1st	07:03	16:57	9.9	280.9	380	18
Spring 1st	06:02	17:58	11.9	456	330	8.85
Summer 1st	04:50	19:10	14.3	525.2	280	6.3

Here the mass flow rate for the three designated days is shown in Fig. 7. The flow rate during the first day of summer increases from 0.025 at 6 am to 0.2 kg/s at noon. Similar trend with higher peaks is observed for the first days of spring and summer.

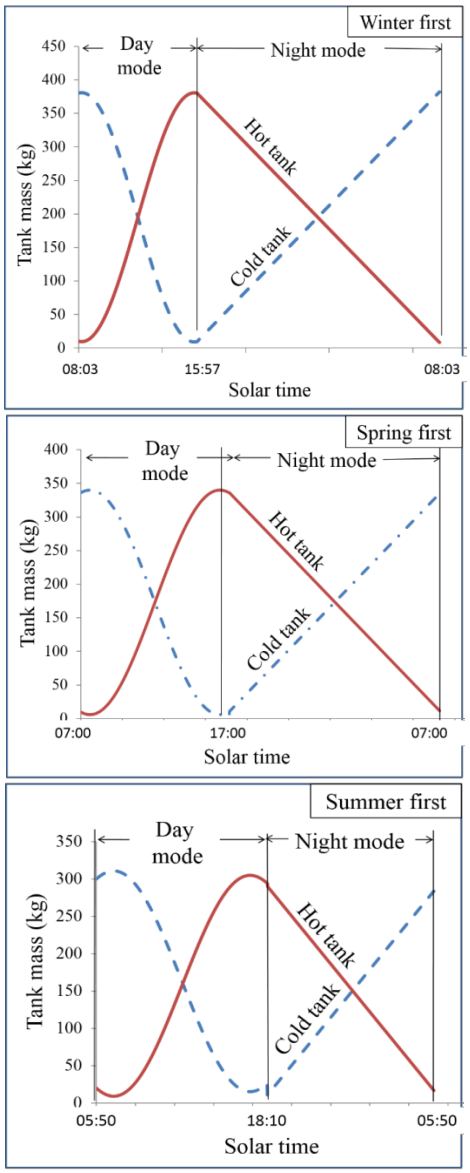

Fig. 6. Heat storage tank mass during day and night for the firsts of winter, spring and summer.

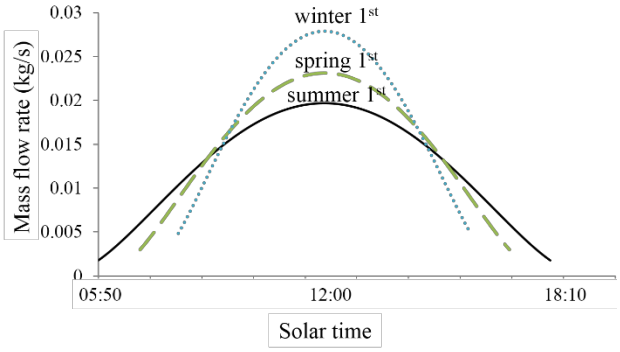

Fig. 7. Mass flow rate to the collector and to the generator during day and night

5. Conclusion

A new comprehensive model, where the "variable with time" nature of sun thermal energy is of concern, is developed. This model is composed of solar collector model with heat storage and absorption refrigerator models. In the temperature range of 215 ^{o}C to 334 ^{o}C with salt melt, an overall collector efficiency of 57.8% is determined experimentally. The direct effects of solar irradiance on refrigerator parameters are predicted well through this model. Because of radiation intensity variations during the day, from around 300 W/m^2 in the morning to more than 900 W/m^2 at noon, the refrigerator's cooling capacity changes. For a 50 W capacity refrigerator with an evaporator temperature of 263 K and a COP of 0.2 at 298.15 K ambient temperature a collector area of 0.3 m^2 to 0.8 m^2 is required. An increase in radiation intensity increases the generator power and temperature. Consequently, the refrigerator's capacity and COP increases. The advantages of a thermal heat storage system in terms of absorbing drastic solar energy change and storing the energy for working overnight and working during cloudy hours are assumed and calculated in a quantitative manner. Applying a thermal heat storage system can overcome the operational drawbacks related to these changes and may assure a steady operation of a solar refrigerator.

Acknowledgements

The fund of this research is provided by Iran Office of Vice-presidency for Science and Technology, Office of Development of Renewable Energy Technologies. The authors thank the supports received from the dean of research at the University of Isfahan. Thanks to Mr Taher Kermani for his help in the experiments.

References

[1] S.A.Said, M.A.El-Shaarawi, M.U.Siddiqui "Alternative designs for a 24-h operating solar powered absorption refrigeration technology", International Journal of Refrigeration,vol. 35, pp. 1967-1977, 2012.

[2] B.L.Lostec, N.Galanis, J.Millette "Experimental study of an ammonia-water absorption refrigerator", International Journal of Refrigeration, vol. 35, pp. 2275-2286, 2012.

[3] B.L.Lostec, N.Galanis, J.Millette "Simulation of an ammonia-water absorption refrigerator", Renewable Energy, vol. 60, pp. 269-283, 2013.

[4] A.Benhmidene, K.Hidouri, B.Chaouachi, S.Gabsi, M.Bourouis "Experimental investigation on the flow behaviour in a bubble pump of diffusion absorption refrigeration systems", Case Studies in Thermal Engineering,vol. 8, pp. 1-9, 2016.

[5] C.Tzivanidis, E.Bellos "The use of parabolic trough collectors for solar cooling – A case study for Athens climate", Case Studies in Thermal Engineering, vol. 8, pp. 403–413, 2016.

[6] A.Zohar, M.Jelinek, A.Levy, I.Borde "Numerical investigation of a diffusion absorption refrigeration cycle", International Journal of Refrigeration, vol. 28, pp. 515-525, 2005.

[7] D.Kong, J.Liu, L.Zhang, H.He, Z.Fang "Thermodynamic and experimental analysis of an ammonia-water absorption refrigerator", Energy and Power Engineering, vol. 2, pp. 298-305, 2010.

[8] M.Ozorgen, M.Bilgili, O.Babayigit "Hourly performance prediction of ammonia-water solar absorption refrigeration", Applied Thermal Engineering, vol. 40, pp. 80-90, 2012.

[9] M.Helm, K.Hagel, W.Pfeffer, S.Hiebler, C.Schweigler "Solar heating and cooling system with absorption chiller and latent heat storage - A research project summary", Energy Procedia, vol. 48, pp. 837 – 849, 2014.

[10] R.Winston, L.Jiang, B.Widyolar "Performance of a 23KW solar thermal cooling system employing a double effect absorption chiller and thermodynamically efficient non-tracking concentrators", Energy Procedia , vol. 48, pp. 1036 – 1046, 2014.

[11] M.Berger, M.Weckesser, C.Weber, J.Döll, A.Morgenstern, A.Häberle "Solar driven cold rooms for industrial cooling applications", Energy Procedia, vol. 30, pp. 904 – 911 , 2012.

[12] B.Pablo, F.J.Pino, F.Rosa "Solar absorption cooling plant in Seville", Solar Energy, vol. 84, pp. 1503–1512, 2010.

[13] A.Al-Alili, M.D. Islam, I.Kubo, Y.Hwang, R.Radermacher "Modeling of a solar powered absorption cycle for Abu Dhabi", Applied Energy, vol. 93, pp. 160–167, 2012.

[14] F.Hosseini, B.Mostajeran Goortani, M.Niroomand "Instantaneous responses of on-grid PV plants to changes in environmental and weather conditions", International Journal of Renewable Energy Research, vol. 6, pp. 1296-1306, 2016.

[15] Y.Agrouaz, T.Bouhal, A.Allouhi, T.Kousksou, A. Jamil, Y.Zeraouli "Energy and parametric analysis of solar absorption cooling systems in various Moroccan climates", Case Studies in Thermal Engineering, vol. 9, pp. 28-39, 2017.

[16] F. Solak, H. Gözde, M.A. Şenol, M.C.Taplamacioglu, Design of power control unit for heat recovery device used in renewable energy system, International Conference on Renewable Energy Research and Applications (ICRERA), 2015, San Diego, USA.

[17] B.Mostajeran, A.Gaurav, A.Deshpande, F.T.T.Ng, G. Rempel "Production of isooctane from isobutene: energy integration and carbon dioxide abatement via catalytic distillation", Industrial and Engineering Chemical Research,vol. 54, pp. 3570–3581, 2015.

[18] G.J.Schmitz, P.Ulrich " Handbook of software solutions for ICME", Wiley-VCH, 380 (2017).

[19] J. A.Duffie, W. A.Beckman "Solar Engineering of Thermal Processes", 4thed, Wiley Publishing Co., (2013).

[20] K. Qiu, E. Thorsteinson, An organic Rankine cycle system for solar thermal power applications, International Conference on Renewable Energy Research and Application (ICRERA), 19-22 Oct 2014, Milwaukee, USA.

[21] M.Ashjaee, M.R.Roomina, A.Ghafouri "Diffuse and global solar radiation for various cities in Iran by two methods and their comparison with the measured data", Solar Energy, vol. 50, pp. 441-446, 1993.

[22] C.A.Gueymard "Clear-sky irradiance predictions for solar resource mapping and large-scale applications: Improved validation methodology and detailed performance analysis of 18 broadband radiative models", Solar Energy, vol. 86, pp. 2145–2169, 2012.

[23] F.P.Incorpera, D.P. DeWitt "Fundamentals of Heat and Mass Transfer", 3rd edition (1990), 658–660. Wiley, New York.

[24] A.Busso, J.Franco, N.Sogari, M.Caceres "Attempt of integration of a small commercial ammonia-water absorption refrigeration with a solar concentrator: Experience and results", International Journal of Refrigeration, vol. 34, pp. 1760-1775, 2011.

[25] T. Salimian, B. Mostajeran Goortani, S.T. Kermani "Conventional Methods of Defining Intensity of Solar Radiation on Horizontal Surface", Renewable Energy Magazine (jrenew), 4(1), 16-21 (summer 2017). (inPersian)

[26] B.Mostajeran Goortani, S.T. Kermani "Solar concentrated energy supply to water-ammonia absorption refrigerators", Proceedings of the 4th International Conference of Fluid Flow, Heat and Mass Transfer (FFHMT'17), Toronto, Canada (Aug. 22, 2017).

[27] Messadi, Y. Timoumi, Modeling of the Parabolic Trough Solar Field with Molten Salt for the Region of Tozeur in Tunisia, International Conference on Renewable Energy Research and Application (ICRERA), 14-19 Oct 2018, Paris, France.

[28] C. Naranjo-Mendoza, D. R. Rousse, G. Quesada, Modeling of a solar absorption cooling system for Guayaquil, Ecuador, 2nd International Conference on Renewable Energy Research and Applications, Madrid, Spain, 20-23 October 2013.

[29] B. Martinkauppi, T. Syrjälä, A. MiKiranta, E. Hiltunen, Some Aspects of Recycling Concrete Crush for Thermal Heat Storage, International Conference on Renewable Energy Research and Application (ICRERA), 14-19 Oct 2018, Paris, France.

[30] M.H. Ahmed, M. Rady, A.M. Amin, F.M. Montagnio, F. Paredes, Comparison of thermal and optical performance of Linear Fresnel and Parabolic Trough Concentrator, International Conference on Renewable Energy Research and Application (ICRERA), 2015, San Diego, USA.